THE JOURNAL OF BIOLOGICAL CHEMISTRY
Vol. 271, No. 37, Issue of September 13, pp. 22346–22351, 1996

Printed in U.S.A.

Activation Mechanism of Methanol:5-Hydroxybenzimidazolylcobamide Methyltransferase from *Methanosarcina barkeri**

(Received for publication, December 29, 1995, and in revised form, June 7, 1996)

Piet J. H. Daas‡, Wilfred R. Hagen§, Jan T. Keltjens‡¶, Chris van der Drift‡, and Godfried D. Vogels‡

From the ‡Department of Microbiology, Faculty of Science, University of Nijmegen, Toernooiveld, NL-6525 ED Nijmegen, The Netherlands and the §Department of Biochemistry, Agricultural University, NL-6703 HA Wageningen, The Netherlands

Methanol:5-hydroxybenzimidazolylcobamide methyltransferase (MT_1) is the first of two enzymes involved in the transmethylation reaction from methanol to 2-mercaptoethanesulfonic acid in *Methanosarcina barkeri*. MT_1 only binds the methyl group of methanol when the cobalt atom of its corrinoid prosthetic groups is present in the highly reduced Co(I) state. Formation of this redox state requires H_2, hydrogenase, methyltransferase activation protein, and ATP. Optical and electron paramagnetic resonance spectroscopy studies were employed to determine the oxidation states and coordinating ligands of the corrinoids of MT_1 during the activation process. Purified MT_1 contained 1.7 corrinoids per enzyme with cobalt in the fully oxidized Co(III) state. Water and N-3 of the 5-hydroxybenzimidazolyl base served as the upper and lower ligands, respectively. Reduction to the Co(II) level was accomplished by H_2 and hydrogenase. The cob(II)amide of MT_1 had the base coordinated at this stage. Subsequent addition of methyltransferase activation protein and ATP resulted in the formation of base-uncoordinated Co(II) MT_1. The activation mechanism is discussed within the context of a proposed model and compared to those described for other corrinoid-containing methyl group transferring proteins.

Methanosarcina barkeri can utilize methanol as sole source for methanogenesis and growth. The first step in the reduction of methanol to methane is the formation of an enzyme-bound methylcobamide catalyzed by methanol:5-hydroxybenzimidazolylcobamide methyltransferase (MT_1)[1] (1). The methyl group of methylated MT_1 is subsequently transferred to 2-mercaptoethanesulfonic acid (coenzyme M, HS-CoM) by Co-methyl-5-hydroxybenzimidazolylcobamide:HS-CoM methyltransferase (MT_2) (2). As a result methyl-coenzyme M (CH_3-S-CoM) is produced, which is the substrate for the final step in methanogenesis in all methanogens studied so far (3).

The corrinoid prosthetic group of MT_1 can only be methylated by methanol when the central cobalt atom of the cobamide is present in the highly reduced Co(I) state (4, 5). Since this state is extremely sensitive toward oxidation, MT_1 readily inactivates upon manipulation and even during catalysis. Reactivation is possible and requires participation of a reducing system, methyltransferase activation protein (MAP), and ATP (4, 6–8). The reducing system consists of hydrogen, hydrogenase, and ferredoxin. Ferredoxin is not absolutely required, though it stimulates the apparent reaction rate of methyl group transfer (6).

Here, we report the UV-visible absorbance and electron paramagnetic resonance properties of the corrinoid prosthetic groups of MT_1 under various additions of the reducing system, MAP, and ATP. From these results, the sequence of events leading to the formation of the cob(I)amide of MT_1 is deduced. The activation of MT_1 proceeds by a novel mechanism, which is presented in a model and compared to those described for other corrinoid-containing methyl group-transferring proteins.

EXPERIMENTAL PROCEDURES

Cell Material—Cells of *M. barkeri* strain MS (DSM 800) were grown and harvested, and cell extract was prepared anaerobically as described previously (6, 9).

Enzyme Assays—Incubation mixtures were prepared in an anaerobic glove box, and reactions were performed in crimp-sealed 10-ml serum vials. MT_1 activity was determined by measuring the methanol-dependent HS-CoM conversion to CH_3-S-CoM when added to a reaction mixture containing MT_2/hydrogenase, MAP, and ferredoxin fractions obtained after DEAE-Sepharose fractionation of cell extract of *M. barkeri* (6). A typical reaction mixture (final volume, 100 μl) contained 50 mM TES/K^+ buffer (pH 7.0), 24 mM $MgCl_2$, 10 mM methanol, 10 mM HS-CoM, 2 mM ATP, 1 mM 2-bromoethanesulfonic acid, 20 μl of MT_2/hydrogenase fraction, 5 μl of ferredoxin fraction, 25 μl of MAP fraction, and an amount (usually 25 μl) of MT_1 to be tested (6). After gassing with 50% H_2, 50% N_2 (100 kPa), the vials were kept on ice. Reactions were started by placing the vials at 37 °C. After appropriate incubation periods, routinely 0, 15, 30, 45, and 60 min, reactions were stopped by placing the vials on ice. Activity of methyl group transfer of methanol to HS-CoM was routinely assayed by measuring the decrease in the amount of HS-CoM (see below). The methyltransferase activity obtained was linearly dependent on the amount of MT_1 added.

The enzymatic activities of MT_2, MAP, hydrogenase, and ferredoxin were determined as described previously (4, 6, 8).

Protein Purification—Because several of the enzymes involved in the methanol:HS-CoM methyltransferase reaction are oxygen-labile (1, 4, 6, 8), all handlings were performed in an anaerobic glove box (97.5% N_2, 2.5% H_2) at room temperature. The purification procedure started by applying 10 ml of cell extract to a DEAE-Sepharose-CL-6B column and separating the proteins involved in the methyltransferase reaction as described previously (6). MT_2 and hydrogenase activity eluted between 0.20 and 0.22 M NH_4Cl. Fractions between 0.25 M and 0.34 M NH_4Cl

* The costs of publication of this article were defrayed in part by the payment of page charges. This article must therefore be hereby marked "*advertisement*" in accordance with 18 U.S.C. Section 1734 solely to indicate this fact.

¶ To whom correspondence should be addressed. Tel.: 31-24-3653437; Fax: 31-24-3553450; E-mail: jankel@sci.kun.nl.

[1] The abbreviations used are: MT_1, methanol:5-hydroxybenzimidazolylcobamide methyltransferase; CH_3-S-CoM (methyl-coenzyme M), 2-(methylthio)ethanesulfonic acid; HS-CoM (coenzyme M), 2-mercaptoethanesulfonic acid; MT_2, Co-methyl-5-hydroxybenzimidazolylcobamide:HS-CoM methyltransferase; MAP, methyltransferase activation protein; CHAPS, 3-[(3-cholamidopropyl)dimethylammonio]-1-propanesulfonate; PAGE, polyacrylamide gel electrophoresis; TES, *N*-tris-(hydroxymethyl)methyl-2-aminoethanesulfonic acid; HBI, 5-hydroxybenzimidazolyl; B_{12}-HBI, 5-hydroxybenzimidazolylcobamide; CAPS, 3-(cyclohexylamino)-1-propanesulfonic acid; kPa, kilopascal(s).

TABLE I
Purification of methanol:5-hydroxybenzimidazolylcobamide methyltransferase

The purification procedure started from 10 ml of cell extract. Enzyme assays were performed as described under "Experimental Procedures." Units are expressed as micromoles of 2-mercaptoethanesulfonic acid methylated per min.

Step	Total protein	Total activity	Specific activity	Factor	Recovery
	mg	*units*	*units/mg*	*-fold*	*%*
Cell extract	260	44.20	0.17	1	100
DEAE-Sepharose	4.4	16.98	3.86	23	38
TSK DEAE	0.6	3.34	5.57	33	8

contained MAP activity. MT_1 was present in fractions eluting between 0.39 and 0.42 M NH_4Cl and ferredoxin was obtained between 0.50 and 0.56 M NH_4Cl. MT_2/hydrogenase, MAP, and MT_1 fractions were washed by Amicon YM-10 ultrafiltration with 50 mM TES/K^+ buffer (pH 7.0) containing 15 mM $MgCl_2$ and 1 mM dithiothreitol to remove the salt, and were concentrated to a final volume of 3, 6, and 1 ml, respectively. Ethylene glycol was added as a stabilizing agent in a final concentration of 10% (v/v). Ferredoxin was washed by Amicon YM-3 ultrafiltration and concentrated to a volume of 3 ml. Here, ethylene glycol was added in a final concentration of 20%.

MT_1 was purified to homogeneity with an anaerobic Perkin-Elmer fast protein liquid chromatography system equipped with a TSK DEAE-5-PW column (7.5 cm by 0.75 cm). After application of a 550-μl DEAE-Sepharose MT_1 fraction, the column was washed with 15 ml of 50 mM TES/K^+ buffer (pH 7.0) containing 15 mM $MgCl_2$, 1 mM dithiothreitol, and 10% ethylene glycol followed by a 113-ml linear gradient of 0–0.25 M NH_4Cl in the buffer. Subsequently, the column was washed with 15 ml of 0.5 M NH_4Cl in the buffer to remove all bound proteins. The eluate was monitored at 280 nm, and fractions of 0.9 ml were collected at a flow rate of 0.45 ml min^{-1}. MT_1 activity was present in a large peak that was eluted at about 0.20 M NH_4Cl. Fractions eluting between 0.18 and 0.22 M NH_4Cl were pooled. This purification step was repeated for the remainder of the DEAE-Sepharose MT_1 fraction. The purified MT_1 pools were combined, washed, and concentrated by Amicon YM-10 ultrafiltration to the desired volume, usually 0.4 ml.

MAP was partially purified on a hydroxylapatite column packed with TSK-Gel HA-1000 (7.5 by 0.75 cm) and equilibrated in 50 mM TES/K^+ buffer (pH 7.0) containing 1 mM dithiothreitol, 0.5 mM CHAPS, and 10% ethylene glycol. After application of the sample (1 ml), the column was washed with 15 ml of equilibration buffer. Bound protein was eluted by a 50-ml simultaneous linear gradient of 50–0 mM TES/K^+ and 0–300 mM ammonium phosphate buffer (pH 7.0); both buffers contained 1 mM dithiothreitol, 0.5 mM CHAPS, and 10% ethylene glycol. Fractions (0.9 ml) were collected at a flow rate of 0.45 ml min^{-1}. MAP activity was recovered in a peak that was eluted at 145 mM ammonium phosphate and 26 mM TES. The purification step was repeated for the remainder of the DEAE-Sepharose MAP fraction. Purified MAP pools were combined, desalted, and concentrated by Amicon YM-10 ultrafiltration by washing with 50 mM TES/K^+ buffer (pH 7.0) containing 1 mM dithiothreitol and 10% ethylene glycol. At this stage, MAP was purified 23-fold with a recovery of 6.5%; apart from MAP (60 kDa) 8–25% native polyacrylamide gel electrophoresis (PAGE) showed the presence in amounts approximately equal to MAP of two contaminating proteins (96 and 32 kDa) that apparently are not related with the methanol:HS-CoM methyltransferase reaction (8). Since the procedure to isolate homogeneous MAP gave very low yields (8), the two-step purification method was employed to obtain the activation protein in the large amounts required for the experiments described.

In order to remove fortuitous Mn^{2+} that interfered with the EPR experiments, MT_2/hydrogenase and ferredoxin fractions were applied separately to a Sep-Pak CM cation exchange cartridge and eluted with 50 mM TES/K^+ buffer (pH 7.0) containing 1 mM dithiothreitol and 10% ethylene glycol.

Analytical Procedures—UV-visible light absorption spectra were recorded in 1-ml quartz cuvettes on a Hitachi U-3200 spectrophotometer. Spectra of MT_1 were recorded against a reference that contained the same components except MT_1. EPR spectroscopy was carried out on a Bruker 200 D spectrometer equipped with cryogenics, peripheral equipment, and data acquisition/manipulation facilities as described previously (10). Incubation mixtures were anaerobically transferred to EPR tubes under a slight overpressure of hydrogen, and directly frozen in liquid nitrogen. EPR spectra of controls containing the same components except MT_1, were also recorded and subtracted from the spectra of the MT_1-containing samples. In the controls MT_1 was replaced by TES/K^+ buffer. EPR spectra were simulated by using the program KOPER (11–13).

Native PAGE, denaturing SDS-PAGE, and isoelectric focusing were performed with prefabricated minigels using the Pharmacia PhastSystem equipment (Uppsala, Sweden). The gels were stained with Coomassie Brilliant Blue R-250. The subunit molecular weight of MT_1 was determined by electrophoresis on a 10–15% gradient minigel with SDS-buffer strips. The markers (Bio-Rad) were the following (Da): α-lactalbumin (14,400), soybean trypsin inhibitor (21,500), bovine carbonic anhydrase (31,000), hen egg white lysozyme (45,000), bovine serum albumin (66,200), and rabbit muscle phosphorylase *b* (97,400). Native PAGE was performed on a 8–25% gradient minigel. Isoelectric focusing was performed with a pH 3–9 isoelectric focusing gel using the pI 3.5–9.6 isoelectric focusing standard proteins from Bio-Rad.

Protein was determined with the Bio-Rad protein reagent with bovine serum albumin as a standard. Molar concentrations of MT_1 were calculated from the molecular mass (122,000 Da) of the protein (1). Molar amounts of hydroxylapatite-purified MAP were estimated from the reported M_r = 60,000 of the protein, taking into account that approximately one-third of the total protein was MAP (8). Corrinoids were quantified after conversion into the dicyanocobamide derivatives. Samples of MT_1 were diluted in 50 mM CAPS buffer (pH 10) containing 5 mM potassium cyanide and incubated for 5 min at 90 °C (14). Concentrations were calculated from the absorption at 580 nm (ϵ_{580} = 10.2×10^3 M^{-1} cm^{-1}) (15). High performance liquid chromatography analysis of corrinoids was performed as described before (6). HS-CoM was measured by the method of Ellman (16). Samples of 25 μl were mixed with 3 ml 0.48 mM 2,2′-dinitro-5,5′-dithiobenzoic acid in 150 mM Tris/Cl^- buffer (pH 8.0) and immediately measured at 412 nm. Total iron was determined as described by Fish (17). Manganese was measured as described by Bartley and co-workers (18). The effect of bathophenanthroline disulfonate was tested anaerobically essentially as described by Rouvière and Wolfe (19).

Materials—All chemicals used were of analytical grade. HS-CoM, 2-bromoethanesulfonic acid, TES, CAPS, bathophenanthroline disulfonate, and hexokinase (yeast type VI) were purchased from Sigma. Dithiothreitol was from Serva Feinbiochemica (Heidelberg, Germany). ATP, CHAPS, and myokinase (adenylate kinase) were purchased from Boehringer (Mannheim, Germany). DEAE-Sepharose-CL-6B was from Pharmacia LKB Biotechnology AB (Uppsala, Sweden). TSK DEAE-5-PW and TSK-Gel HA-1000 columns were obtained from TosoHaas (Stuttgart, Germany). Sep-Pak CM cartridges were acquired from Waters Associates (Milford, MA). Gasses were supplied by Hoek-Loos (Schiedam, The Netherlands). To remove traces of oxygen, H_2-containing gases were passed over a BASF RO-20 catalyst at room temperature; nitrogen was passed over a prereduced BASF R3–11 catalyst at 150 °C. The catalysts were a gift of BASF Aktiengesellschaft (Ludwigshafen, Germany).

RESULTS

Purification of MT_1—Methanol:5-hydroxybenzimidazolylcobamide methyltransferase was purified to homogeneity from cell extract of *M. barkeri* strain MS by the simple two-step procedure summarized in Table I. After this stage only one band was detected upon nondenaturing 8–25% gradient PAGE showing an apparent M_r = 121,000 (Fig. 1). Superose-6 chromatography indicated a molecular mass of about 120 kDa. These values favorably agree with the M_r = 122,000 described before (1). Prior to staining of the gel, the protein could be observed as a red-colored band indicative of the presence of corrinoids. Denaturating SDS-PAGE demonstrated the $\alpha_2\beta$ subunit composition of polypeptides of 33,000 and 54,000, respectively, as described before (1). With the protein determination employed (Bio-Rad), an average 1.7 ± 0.4 mol of 5-hydroxybenzimidazolylcobamide (B_{12}-HBI)/mol of MT_1 was

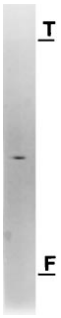

FIG. 1. **Polyacrylamide gel electrophoresis of purified methanol: 5-hydroxybenzimidazolylcobamide methyltransferase (MT_1).** A 4-μl sample (2.0 μg of protein) was applied to a 8–25% Gradient Phastgel and stained with Coomassie Brilliant Blue. *T*, top; *F*, front.

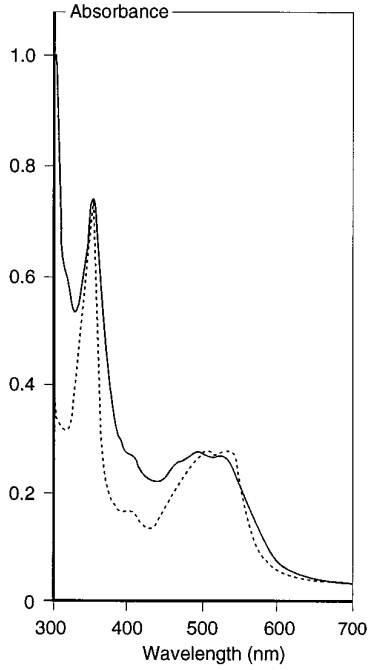

FIG. 2. **Absorption spectrum of purified MT_1.** The spectrum of MT_1 (0.82 ml; 2.5 mg/ml; 20.6 μM) was recorded in an anaerobic 1-ml quartz cuvette at 37 °C under 50% H_2/50% N_2 in 50 mM TES/K^+, pH 7.0, containing 15 mM $MgCl_2$, 1 mM dithiothreitol, and 10% ethylene glycol (——). The spectrum of non-protein-bound Co-aquo-5-hydroxybenzimidazolylcobamide (aquo-B_{12}-HBI) (26 μM) was recorded in the same buffer (- - -).

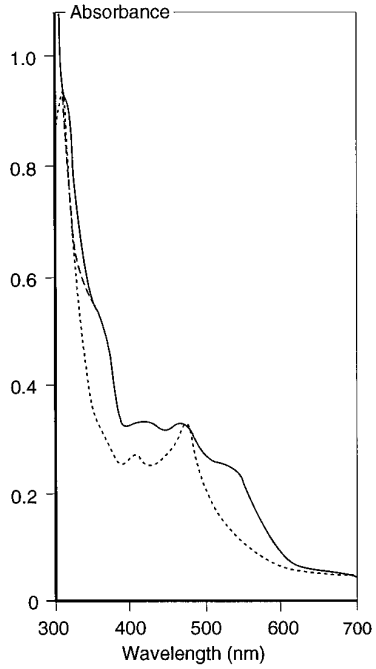

FIG. 3. **Absorption spectrum of hydrogen-reduced MT_1.** Spectra were recorded as described in Fig. 2. Absorption spectrum of MT_1 (0.82 ml; 2.5 mg/ml; 20.6 μM) after incubation for 90 min at 37 °C in the presence of 12 μl of MT_2/hydrogenase and 8 μl of ferredoxin fraction (*full line*) and the subsequent addition of MAP (20 μM) and ATP (2.5 mM) (*long dashes*). The spectrum of the cob(II)amide (- - -) was obtained after reduction of aquo-B_{12}-HBI (33 μM) under the same conditions.

determined from three separate purifications. We found that the presence of Mg^{2+} (15 mM) in the buffer systems was a prerequisite in the isolation of MT_1. Treatment of MT_1 preparations with 50 mM EDTA, which removed Mg^{2+}, and subsequent native PAGE showed the loss of the corrinoid prosthetic group and a dissociation of the protein (not shown). Apparently, Mg^{2+} plays a role in binding of the corrinoid prosthetic group and in subunit association. From isoelectric focusing, a pI of 4.5 was obtained. Determination of non-heme iron revealed the presence of 1.7 mol of Fe/mol of MT_1; acid-labile sulfur could not be detected. Pretreatment with 2 mM of the iron chelator bathophenanthroline disulfonate did not result in any loss of activity. In addition, EPR spectroscopy studies of MT_1 at 14 K, in the absence and presence of 2 mM dithionite, did not reveal any signals indicative of the presence of iron-sulfur clusters. From this, it was concluded that MT_1 does not contain functionally active iron.

UV-visible Spectroscopy—MT_1 was anaerobically isolated as a red-colored protein. The UV-visible spectrum of the prosthetic group (Fig. 2) was typical of Co(III) corrinoids (20–22). Exposure to air did not further alter the spectrum. The prosthetic group showed absorption maxima at 352 (2.89), 493 (1.07), and 522 (1.04) nm with shoulders at 388 (1.16), 403 (1.04), and 465 (1.0) nm (the numbers in parentheses express the absorbance relative to that of the shoulder at 465 nm). The major visible absorption band at 352 nm is characteristic of the presence of water as the upper ligand (21, 22). Compared to free aquo-B_{12}-HBI, the absorbance of the corrinoid of MT_1 was relatively increased in the 375–475 nm region. Incubation of purified cob(III)amide-MT_1 with up to equimolar amounts of MAP and/or ATP (up to 5 mM) had no effect on the UV-visible spectrum of the corrinoid prosthetic groups.

When MT_1 was incubated under hydrogen with a small amount of MT_2/hydrogenase and ferredoxin, the protein turned yellow. The spectrum (Fig. 3) displayed the typical characteristics of cob(II)amide (5, 20, 21). Absorption maxima were observed at 417 (1.31) and 465 (1.29) nm with shoulders at 315 (3.64), 356 (2.11), and 535 (1.0) nm (the numbers in parentheses indicate the absorbance relative to that of the shoulder at 535 nm). Compared to the spectrum of free Co(II) B_{12}-HBI, the Co(II) prosthetic group of MT_1 exhibited a relative increase in the absorbances around 400 nm and in the 500–600 nm regions. Prolonged incubation or the addition of higher amounts of hydrogenase and ferredoxin did not result in any alterations of the spectrum. Ferredoxin was not absolutely required for the reduction.

The spectrum of the hydrogen-reduced Co(II) form of MT_1 was not altered by the subsequent addition of MAP, ATP, or methanol alone. When both MAP and ATP were added the shoulder at 315 nm of the cob(II)amide of MT_1 disappeared while no significant changes occurred at higher wavelengths (Fig. 3). Interestingly, a distortion of the absorbance band at 315 nm is the major feature, when the HBI nucleotide in free Co(II) B_{12}-HBI becomes decoordinated ("base-off") upon acidi-

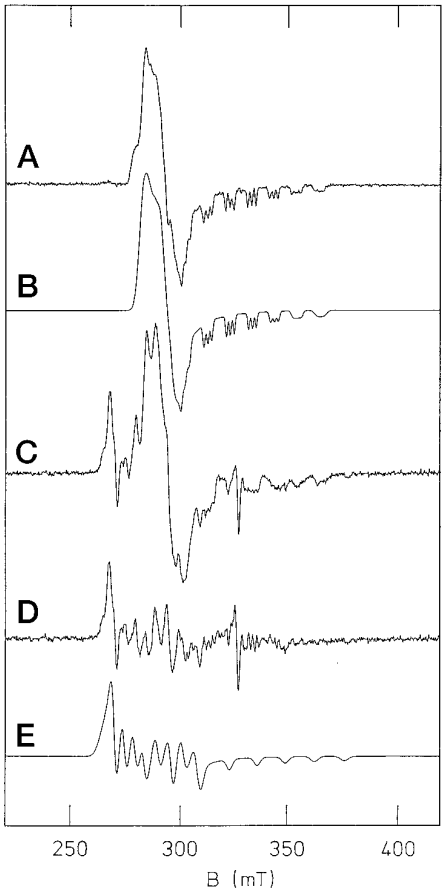

FIG. 4. **Low spin Co(II) EPR spectra of MT_1.** The corrinoids of MT_1 were reduced to the Co(II) level with hydrogenase and ferredoxin as described under Fig. 2 followed by storage for 16 h at 4 °C. *Trace A*, 2 × averaged spectrum of the base-on form of Co(II) MT_1 (35 mg/ml; 287 μM). *Trace B*, simulation of *A*. *Trace C*, 9 × averaged, base-line corrected spectrum of Co(II) MT_1 (1.93 mg/ml; 15.8 μM) obtained after incubation with MAP (0.45 mg/ml; 7.5 μM), ATP (5 mM), and $MgCl_2$ (7.5 mM) for 90 min at 37 °C under 5% H_2/95% N_2; the spectrum shows that part of the MT_1 is still in the base-on form. *Trace D*, difference spectrum of *C* minus *A*. *Trace E*, simulation of *D*. See "Results" and Table II for details on the simulations. EPR conditions: microwave frequency, 9.18 GHz; modulation frequency, 100 kHz; modulation amplitude, 0.63 (*trace A*) and 0.8 millitorr (trace *C*); microwave power, 0.08 (*trace A*) and 0.32 milliwatts (*trace C*); temperature, 24 K (*trace A*) and 19 K (*trace C*).

fication (21). When MT_1 was incubated in the presence of the reducing system (H_2, hydrogenase, ferredoxin), MAP and ATP, we never detected the characteristic absorption peak of cob(I)amide at 390 nm. However, the additional presence of methanol in even low concentrations (<100 μM) resulted in the instantaneous formation of methyl-B_{12}-HBI as found by high performance liquid chromatography analysis of the extracted corrinoids (data not shown; see also Ref. 6).

EPR Spectroscopy—EPR observations of corrinoids are limited to the paramagnetic Co(II) state of cobalt. Thus, the purified, cob(III)amide-containing MT_1 was EPR-silent. After incubation of MT_1 with hydrogenase and ferredoxin under hydrogen the typical signal of the nucleotide base-coordinated ("base-on") form of Co(II) corrinoids (Fig. 4*A*) was observed (23). The spectrum could be simulated on the basis of a near-axial, low spin Co(II) complex with hyperfine splitting from the I = 7/2 cobalt nucleus and superhyperfine splitting from an axially coordinating nitrogen with I = 1 (Table II and Fig. 4*B*). For a reasonable fit, it was required that the line width in the z-direction was a function of the cobalt nuclear quantum number m_I. In the perpendicular (or *xy*-) direction, there was no resolution. Therefore, the combined *xy* values for g, A, and W were not uniquely determined. However, it was found by extensive fitting that the low field shoulder to the experimental spectrum could not be simulated by any combination of these parameters. This shoulder might well be a manifestation of non-collinearity of the g and A(Co) tensors, *i.e.* the actual symmetry of the coordination site was probably triclinic.

TABLE II
Simulation parameters for the low spin Co(II) EPR spectra of MT_1

Powder patterns were generated from 201 × 11 molecular orientations. The spin Hamiltonian was $H = \beta BgS + SA_{Co}I + SA_NI$. W_o is the width of a Gaussian in magnetic field space, and the line width was a function of the central nuclear quantum number m_I according to $W = W_o + Bm_I + C(m_I^2$. All tensors g, A_{Co}, A_N, W_o, B, and C are taken to be collinear.

Tensor	Orientation		
	(*x*)	(*y*)	(*z*)
Base-on form			
g	2.26	2.22	2.01
A_{Co} (mT)	0.5	0.5	10.4
A_N (mT)	0	0	1.8
W_o (mT)	3.2	3.2	1.6
B	0	0	0.03
C	0	0	0.05
Base-off form			
g	2.32	2.29	2.00
A_{Co} (mT)	5.0	5.3	13.0
W_o (mT)	4.5	2.0	1.7
B	0	0	0.1
C	0	0	0

While the presence of MAP or ATP alone did not alter the EPR spectrum of Co(II) MT_1, the combination of both induced a remarkable change (Fig. 4*C*). The spectrum was now a sum of two Co(II) spectra: a base-on and a base-off spectrum. The cobalt hyperfine splitting of the latter could be seen to extend to higher field values than that of the former. This pattern became somewhat obscured when we subtracted the pure base-on spectrum from the sumspectrum (resulting in *trace D* in Fig. 4). Because of the low signal-to-noise ratio, however, the *xy* pattern of the base-off spectrum was now more easily identified, thus allowing for a simulation of this spectrum (Table II and Fig. 4*E*). From the simulated spectra (Fig. 4, *B* and *E*) and the combined spectrum (Fig. 4*C*) it could be estimated that 38% of the cob(II)amide in MT_1 was base-uncoordinated. Lower concentrations of MAP gave lower amounts of the base-off species. The formation of base-off Co(II) MT_1 indicated that, as the result of the action of MAP and ATP, the HBI-base was no longer coordinated and that no ligand or a weak ligand with poor delocalization properties was present (23).

DISCUSSION

Optical and EPR spectroscopical studies were employed to determine the oxidation state of the central cobalt atom and the coordination of the ligands in the corrinoid protein MT_1 under various additions of MAP, ATP, and a reducing system. After isolation MT_1 contained somewhat less then 2 mol of B_{12}-HBI/mol of $\alpha_2\beta$ protein. The UV-visible light spectrum (Fig. 2) indicated that the prosthetic group was present in the hexacoordinated Co(III) oxidation state with the nucleotide 5-hydroxybenzimidazole and water as the lower and upper ligands, respectively. Purified MT_1 is inactive, and reactivation apparently requires the reduction of Co(III), which is brought about by a reducing system (H_2, hydrogenase, and ferredoxin), MAP, and ATP (4, 6, 8) (Fig. 5). Incubation of MT_1 with hydrogen, hydrogenase, and ferredoxin resulted in the reduction to the Co(II) state. EPR spectroscopy demonstrated that the HBI-base was still coordinated at this stage (base-on). Subsequent addition of both MAP and ATP induced a conversion of base-on

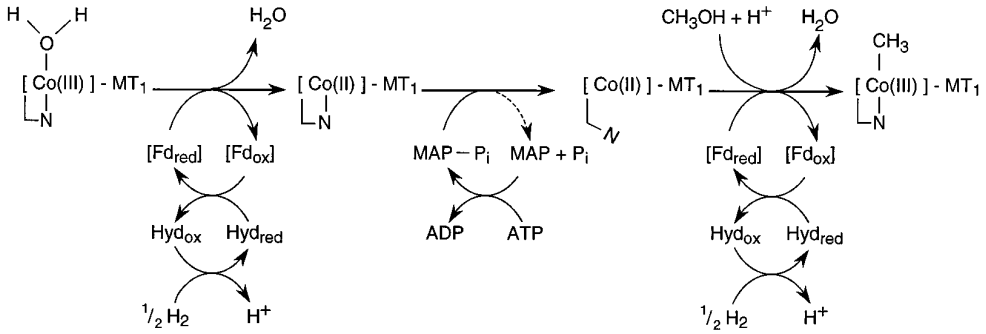

FIG. 5. **Proposed scheme for the reductive activation of MT_1.** [Co(III)] and [Co(II)] represent the various reduction states of the cobalt atom of the corrinoids of MT_1. Coordination of N-3 of the 5-hydroxybenzimidazolyl base is illustrated by the connecting line between Co and N. In the base-off Co(II) state, no ligand is shown but it is possible that a ligand with poor delocalization properties, *e.g.* water, is present. The *dashed line* indicates that it is not fully known how and at which stage MAP-phosphate is dephosphorylated. By the combined action of the reducing system, MAP-phosphate and methanol, catalytically active MT_1 containing methyl-B_{12}-HBI is subsequently produced. *Hyd*, hydrogenase; *Fd*, ferredoxin. Ferredoxin is shown in *parentheses* because activation can occur in the absence of this electron carrier (6).

into base-off Co(II) MT_1. We previously showed MAP to be autophosphorylated by ATP; MAP-phosphate is able to substitute for the requirement of MAP and ATP (8). The phosphorylated protein, thus effects MT_1 in such a way that the HBI-base becomes dissociated. In the experiment shown in Fig. 4, an estimated 38% of the corrinoids became base-uncoordinated when MT_1 (15.8 μM) was incubated with 7.5 μM MAP and excess ATP (5 mM). From this, it follows that the concentration of base-off MT_1 amounted to 6.0 μM, which is about equimolar with respect to MAP added. In agreement with this conclusion, lower amounts of base-off cob(II)amide were obtained when the MAP concentration was decreased in the EPR experiments.

The conversion of base-on into base-off cob(II) amide has an important implication. In non-protein bound B_{12}-HBI, such base-off conversion causes the midpoint redox potential of the Co(II)/Co(I) couple to increase from -592 to -500 mV (21). In a similar way, the action of MAP and ATP may facilitate the reduction in MT_1 of cob(II)amide to the catalytically active species, the powerful nucleophile cob(I)amide. Although we could not detect the direct formation of cob(I)amide in our experiments, the findings that (i) the species is produced upon demethylation of methylated MT_1 (5) and (ii) methyl-B_{12}-HBI bound to MT_1 is formed during the activation of the enzyme in the presence of H_2, hydrogenase, MAP, ATP and methanol (this paper; Refs. 4–6), demonstrate that cob(I)amide must play a role in the catalytic and reductive activation cycles. The cob(II)amide/cob(I)amide midpoint redox potentials are strongly influenced by the protein environment. In the corrinoid/iron-sulfur proteins involved in acetyl-CoA synthesis and degradation that have been isolated from *Clostridium thermoaceticum* (24) and from *Methanosarcina thermophila* (25), reduction to the catalytically active Co(I) state occurred at midpoint redox potentials of −504 mV (26) and −486 mV (25), respectively. Here, reduction has to be performed by electrons derived from the carbonyl (CO)/CO_2 oxidation ($E_0' = -520$ mV). It is important to note that the enzymes do not require ATP for the activation; in the purified, inactive cob(II)amide state, the corrinoids are already contained in the (at neutral pH) thermodynamically unfavorable base-off state by the protein backbone. Here, the observed midpoint redox potentials about equaled the $E_0' = -500$ mV of the free base-off cob(II)amide/cob(I)amide couple. For a number of corrinoid-containing methyltransferases, midpoint potentials have been measured that were significantly higher than found for the corresponding B_{12} derivatives in solution (25–28). For example, the reduction of base-on cob(II)amide to cob(I)amide in the membrane-bound methyltetrahydromethanopterin:HS-CoM methyltransferase complex from *Methanosarcina mazei* showed an E_0' as high as −426 to −450 mV, which is about 150 mV more positive than the analogous reduction of free B_{12}-HBI (28). In comparing the UV-visible light spectra of MT_1 with aqueous solutions of B_{12}-HBI, we noticed some differences in the 400 nm and 500–600 nm regions (Figs. 2 and 3). Since MT_1 does not contain Fe-S clusters (this paper) or other chromophoric groups (results not shown), this had to be caused by a conformational distortion of the corrin ring structure by the protein (29). Such distortion is likely to change the reduction potential of the prosthetic group. Incubation of methyltetrahydromethanopterin:HS-CoM methyltransferase with ATP and the methyl donor (methyltetrahydromethanopterin) raised the apparent midpoint potential another 200 mV ($E_0' = -245$ mV) (28), *i.e.* to a level where reduction becomes feasible at even very low hydrogen concentrations ($E_0' = -414$ mV). Remarkably, the 200 mV shift was not observed when the methyl donor was omitted, and the authors (28) proposed that the simultaneous action of ATP and the methylating substrate in a ternary enzyme complex is required for raising the redox potential. This may also apply to MT_1. As pointed out above, we never observed the characteristic UV-visible light spectral features of cob(I)amide upon incubation under even high (100 kPa) hydrogen partial pressure of MT_1 with MAP and ATP. However, the additional presence of methanol results in the formation of methyl-B_{12}-HBI in MT_1, suggesting a cooperative action of MAP-phosphate and methanol in the reductive activation (Fig. 5). The EPR experiments outlined above indicated that the amount of base-off cob(II) amide formed was dependent on the amount of MAP added. Yet, MT_1 may be fully activated in the presence of substoichiometric amounts of MAP provided ATP and methanol is present (6, 8). This may be explained by assuming that MAP becomes dephoshorylated after completion of the activation cycle of the MT_1 molecule (8) (Fig. 5). Rephosphorylation by ATP then yields MAP-phosphate for activation of another molecule. Future investigations have to clarify questions with respect to the corrinoid midpoint redox potentials in MT_1 and the effects hereon of MAP-phosphate and methanol.

In order to be active, corrinoid-dependent methyltransferases often require an ATP-dependent reductive activation (3, 30). As yet, only the activation mechanism of methionine synthase has been elucidated (31). Here, ATP is the substrate in the formation of the potent methylating agent, *S*-adenosyl methionine, which traps Co(I) out of the thermodynamic unfavorable Co(II) to Co(I) reduction equilibrium (31). In this paper, we have presented evidence that nature developed another approach to facilitate the generation of the active enzymes, notably by inducing in an ATP-dependent process the conformational change of the prosthetic group. Perhaps other corri-

noid-containing methyltransferases from methanogens (3) and other obligate anaerobic organisms (32) are activated in a similar fashion.

Acknowledgments—We thank Jeroen Zandbergen and Steven van den Berg for assistance in the purification and characterization of MT_1. We gratefully acknowledge Roel Wassenaar for skillful determination of the effect of MAP-phosphate.

REFERENCES

1. van der Meijden, P., te Brömmelstroet, B. W., Poirot, C. M., van der Drift, C., and Vogels, G. D. (1984) *J. Bacteriol.* **160,** 629–635
2. van der Meijden, P., Heythuysen, H. J., Pouwels, A., Houwen, F., van der Drift, C., and Vogels, G. D. (1983) *Arch. Microbiol.* **134,** 238–242
3. Keltjens, J. T., and van der Drift, C. (1986) *FEMS Microbiol. Rev.* **39,** 259–303
4. van der Meijden, P., van der Lest, C., van der Drift, C., and Vogels, G. D. (1984) *Biochem. Biophys. Res. Commun.* **118,** 760–766
5. van der Meijden, P., Jansen, L. P. J. M., van der Drift, C., and Vogels, G. D. (1983) *FEMS Microbiol. Lett.* **19,** 247–251
6. Daas, P. J. H., Gerrits, K. A. A., Keltjens, J. T., van der Drift, C., and Vogels, G. D. (1993) *J. Bacteriol.* **175,** 1278–1283
7. van der Meijden, P., Heythuysen, H. J., Sliepenbeek, H. T., Houwen, F. P., van der Drift, C., and Vogels, G. D. (1983) *J. Bacteriol.* **153,** 6–11
8. Daas, P. J. H., Wassenaar, R. W., Willemsen, P., Theunissen, R. J., Keltjens, J. T., van der Drift, C., and Vogels, G. D. (1996) *J. Biol. Chem.* **172,** 22339–22345
9. Hutten, T. J., De Jong, M. H., Peeters, B. P. H., van der Drift, C., and Vogels, G. D. (1981) *J. Bacteriol.* **145,** 27–34
10. Pierik, A. J., and Hagen, W. R. (1991) *Eur. J. Biochem.* **195,** 505–516
11. Jetten, M. S. M., Pierik, A. J., and Hagen W. R. (1991) *Eur. J. Biochem.* **202,** 1291–1297
12. Holliger, C., Pierik, A. J., Reijerse, E. J., and Hagen, W. R. (1993) *J. Am. Chem. Soc.* **115,** 5651–5656
13. Arendsen, A. F., Verhagen, M. F. J. M., Wolbert, R. B. G., Pierik, A. J., Stams, A. J. M., Jetten, M. S. M., and Hagen, W. R. (1993) *Biochemistry* **32,** 10323–10330
14. Ljungdahl, L. G., LeGall, J., and Lee, J.-P. (1973) *J. Biol. Chem.* **12,** 1802–1808
15. Pol, A., van der Drift, C., and Vogels, G. D. (1982) *Biochem. Biophys. Res. Commun.* **108,** 731–737
16. Ellman, G. L. (1958) *Arch. Biochem. Biophys.* **74,** 443–450
17. Fish, W. W. (1988) *Methods Enzymol.* **158,** 357–364
18. Bartley, W., Notton, B. M., and Werkheiser, W. C. (1957) *Biochem. J.* **67,** 291–295
19. Rouvière, P. E., and Wolfe, R. S. (1989) *J. Bacteriol.* **171,** 4556–4562
20. Friedrich, W. (1975) in *Fermente, Hormone, Vitamine* (Ammon, R., and Dirscherl, W., eds) Vol 3/2, pp. 46–70, Georg Thieme Verlag, Stuttgart, Germany
21. Daas, P. J. H., Keltjens, J. T., Hagen, W. R., and van der Drift, C. (1995) *Arch. Biochem. Biophys.* **319,** 244–249
22. Pol, A., Gage, R. A., Neis, J. M., Reijnen, J. W. M., van der Drift, C., and Vogels, G. D. (1984) *Biochim. Biophys. Acta* **797,** 83–93
23. Pilbrow, J. R. (1982) in B_{12} (Dolphin, D., ed) Vol. 1, pp. 431–462, John Wiley & Sons, New York
24. Ragsdale, S. W. (1991) *Crit. Rev. Biochem. Mol. Biol.* **26,** 261–300
25. Jablonski, P. E., Lu, W.-P., Ragsdale, S. W., and Ferry, J. G. (1993) *J. Biol. Chem.* **268,** 325–329
26. Harder, S. A., Lu, W.-P., Feinberg, B. F., and Ragsdale, S. W. (1989) *Biochemistry* **28,** 9080–9087
27. Banerjee, R. V., Harder, S. R., Ragsdale, S. W., and Matthews, R. G. (1990) *Biochemistry* **29,** 1129–1135
28. Lu, W.-P., Becher, B., Gottschalk, G., and Ragsdale, S. W. (1995) *J. Bacteriol.* **177,** 2245–2250
29. Gianotti, C. (1982) in B_{12} (Dolphin, D., ed) Vol. 1, pp. 393–430, John Wiley & Sons, New York
30. Matthews, R. G., Banerjee, R. V., and Ragsdale, S. W. (1990) *Biofactors* **2,** 147–152
31. Banerjee, R. V., and Matthews, R. G. (1990) *FASEB J.* **4,** 1450–1459
32. Diekert, G., and Wohlfarth, G. (1994) *Antonie van Leeuwenhoek* **66,** 209–221